Measuring and Analyzing Contact Hole Variations in EUV Lithography

Joren Severi[a], Gian Francesco Lorusso[a], and Danilo De Simone[a], Chris A. Mack[b]

[a]*imec, Kapeldreef, Leuven, Belgium*
[b]*Fractilia, LLC, 1605 Watchhill Rd, Austin, TX 78703, USA*

Abstract

Background: Decomposing an observed variation in critical dimension (CD) into its sources of variation is an important analysis, but it is often tedious and prone to error. For EUV processes, identifying the magnitude of stochastic variations is especially important and relevant.
Aim: An automated process for decomposing CD errors into its sources will aid in the analysis of a specific EUV process.
Approach: MetroLER offline metrology software has been updated to perform automated sources of variation analysis, including the measurement and subtraction of systematic and random components, such as across-SEM-field signatures and random metrology errors.
Results: For a staggered array of 24 nm contacts holes on an 80x46 nm pitch, the total CD uniformity (CDU) of about 3.3 nm included a global CDU across wafer of about 1.0 nm, a systematic mask contribution of 1.7 nm, systematic metrology contribution of 1.0 nm, and a random metrology contribution of 0.67 nm (all 3σ), leaving a stochastics-only CDU of about 2.6 nm.
Conclusions: Careful consideration of the systematic and random components in CD measurement variations enables measurement of the stochastic contribution to a state-of-the-art EUV contact printing process. The contribution of metrology error is too large to be ignored. Automation of this decomposition helps to ensure the reliability of the results.

Keywords: Sources of variation, stochastics, EUV lithography, contact hole, CD-SEM

I. INTRODUCTION

A "sources of variation" analysis is a common procedure in the semiconductor industry. For example, a specific lithography step will result in an unintended variation in the critical dimension (CD) of specific repeated patterns. A sources of variation study attempts to assign causes (and magnitudes) to the CD variation in order to facilitate control and reduction of this variability. There are two basic approaches that can be used: characterizing output CD variations (a bottoms-up approach) and characterizing input parameter variations (a top-down approach). Analyzing CD data involves the separation of CD errors into random errors (such as stochastic errors and metrology errors) and temporally and/or spatially systematic errors (across-wafer, across-field, slit direction and scan direction, etc.).[1] Systematic variations across some spatial domain (such as across the scanner field) is called a systematic signature.

Historically, systematic spatial variations were dominant and much of the sources of variation analysis was geared towards identifying spatial signatures and their causes. More recently, stochastic errors in leading-edge patterning processes have become greater than systematic errors, creating additional challenges for the sources of variation analysis process.[2,3,4] Separating stochastic errors from other errors (and in particular metrology errors) is thus an important part of the sources of variation analysis today. Additionally, systematic across-SEM-field CD variations are frequently ignored and thus lumped into stochastic variation, inflating those numbers.

A common mathematical approach to a bottoms-up sources of variation study is Analysis of Variance (ANOVA) with a nested design.[5] However, it is important to separate systematic from random errors, dealing

with systematic errors using straight subtraction, whole random errors are removed in quadrature. The main contributors to CD variation are global CD variation (i.e., systematic spatial signatures from all possible sources), local CD variations on the mask (which can become a systematic error depending on the experiment's sampling plan), local CD variations on the wafer not caused by the mask, and random and systematic metrology errors. These so-called "local" variations are considered stochastic if the observed variability is over a very short spatial distance (typically the field of view of one SEM image) so that global variations will not play a significant role, and when the pattern being measured is known to exhibit uniform imaging (no optical proximity effects, for example, such as would be obtained from a very large array of nominally identical features).

While this type of analysis is common, it is rarely automated and sometimes misapplied. The result is a process that is often tedious and prone to (human) error and bias. Further, care must be taken during sampling design if proper separation of components is to be achieved. This study thus has two goals. The first is to develop an automated (or mostly automated) process of performing sources of variation decomposition that relies to a minimum extent on the statistical skills of the person performing the analysis and thus minimizes the chances of error or bias. The second goal is to assess the sources of variation of a specific EUV lithography process for the printing of three pitches of staggered arrays of contact.

II. EXPERIMENTAL CONDITIONS

The sample preparation for EUV exposure was done at imec. In a first step the wafer was subjected to dehydration bake after which a siloxane-based underlayer was coated at 20 nm film thickness and baked. On top of this layer a positive-tone chemically amplified resist was coated and baked to a film thickness of 50 nm. The wafers were subsequently exposed using a full-field NXE:3400 scanner with a custom hexapole illumination and a dark-field mask to achieve a staggered contact hole pattern at various pitches. The three sets of pitches were H80V46 (meaning the pitch in the horizontal direction was 80 nm and the pitch in the vertical direction was 46 nm), H70V40, and H66V38. An exposure dose of 80 mJ/cm^2 and a focus of 0.1 µm was used. Afterwards, the wafers received a post-exposure bake and were developed with a 2.38% tetramethyl ammonium hydroxide (TMAH) solution.

ADI (after develop inspect) patterning images were taken with a Hitachi 6300 CD-SEM. The metrology settings used were the following: 1024x1024 pixel images, at 0.8 nm x 0.8 nm pixel size, 500V, and 16 frames. In a first sampling plan the corner of the array was used for image alignment, and 1 image was collected per field for a total of 144 images for the wafer. In each image 202 contacts were measured, and the exact same location was measured twice, respectively Run 1 and Run 2. In the second sampling plan 50 images were taken at a different location on the central die of the wafer by moving the SEM in the Y-direction away from the edge of the array. All images obtained in sampling plan 1 and 2 were then subjected to an analysis with Fractilia's MetroLER v2.2.5.

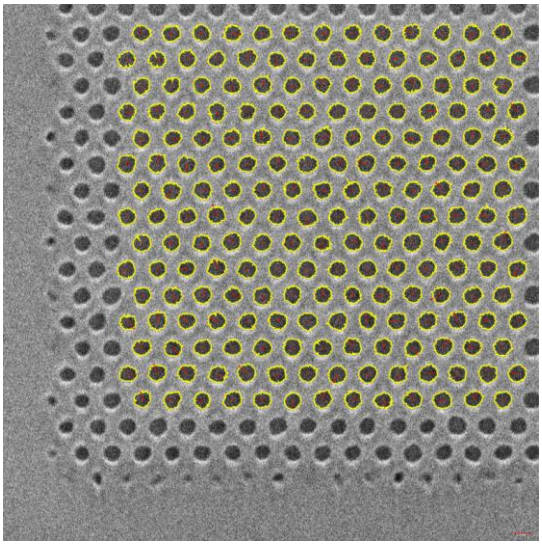

Figure 1. Example of measuring holes at the corner of the array (sampling plan 1) to ensure that the exact same holes are measured each time.

III. ANALYSIS AND DISCUSSION OF RESULTS

For each of the three pitches, 144 SEM images were analyzed as a batch using MetroLER. The automated analysis separates local and global CD variation and can provide across-wafer or across-scanner-field plotting and statistical analysis. The results shown in Figures 2-4 (for the H80V46 pitch) used the first sampling plan (images aligned to the corner of the array), with the same points on the wafer measured twice (Run 1 and Run 2). The total CDU of about 3.3 nm consists of about 1.0 nm of across-wafer global CDU and 3.1 nm of local CDU. Optionally, selecting "subtract SEM distortion signature" will subtract the across-SEM-field signature displayed in Figure 4 before generating the local CD error distribution. Note that for the first sampling plan this across-SEM-field signature includes optical proximity effects, systematic mask variations, and the systematic error signature of the CD-SEM. The resulting local CDU of Figure 5 thus removes mask and CD-SEM systematic errors, giving a local CDU without these systematic errors of about 2.7 nm.

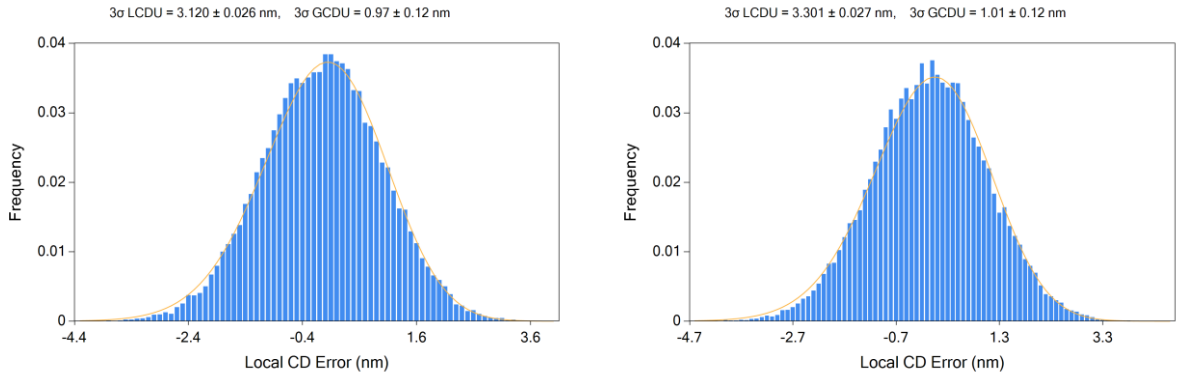

(a) (b)

Figure 2. Histograms of local CDU for (a) Run 1, and (b) Run 2 using the first sampling plan (aligned to the array corner) and horizontal pitch = 80 nm, vertical pitch = 46 nm (H80V46). The local CD error comes from 202 holes measured in one image relative to the mean of that image, then combined with the results from all 144 images.

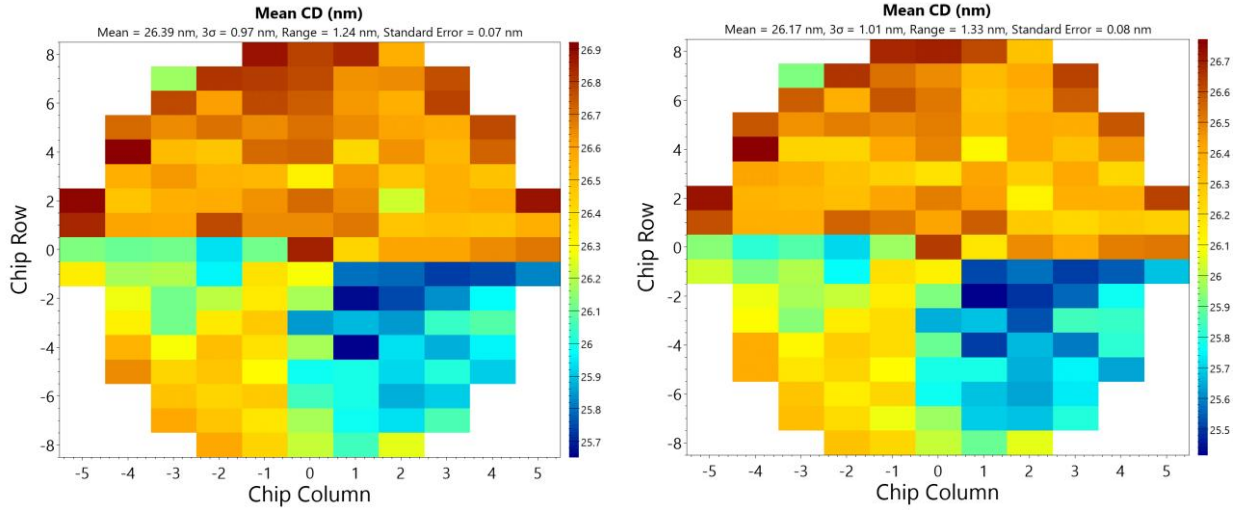

(a) (b)

Figure 3. Across-wafer spatial signatures for (a) Run 1, and (b) Run 2 using the first sampling plan (aligned to the array corner) and horizontal pitch = 80 nm, vertical pitch = 46 nm. Each row/column position value is the mean CD from one image (202 contact holes per image).

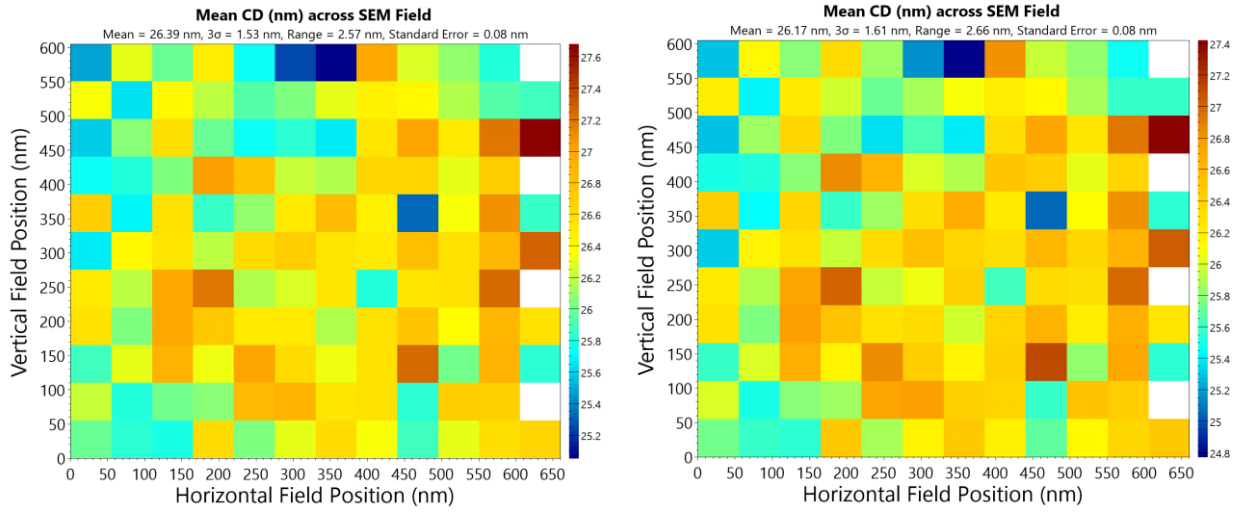

(a) (b)

Figure 4. Across-SEM-field spatial signatures (mask + CD-SEM systematics) for (a) Run 1, and (b) Run 2 using the first sampling plan (aligned to the array corner) and horizontal pitch = 80 nm, vertical pitch = 46 nm. Each point in the SEM field is the average of 144 images across the wafer.

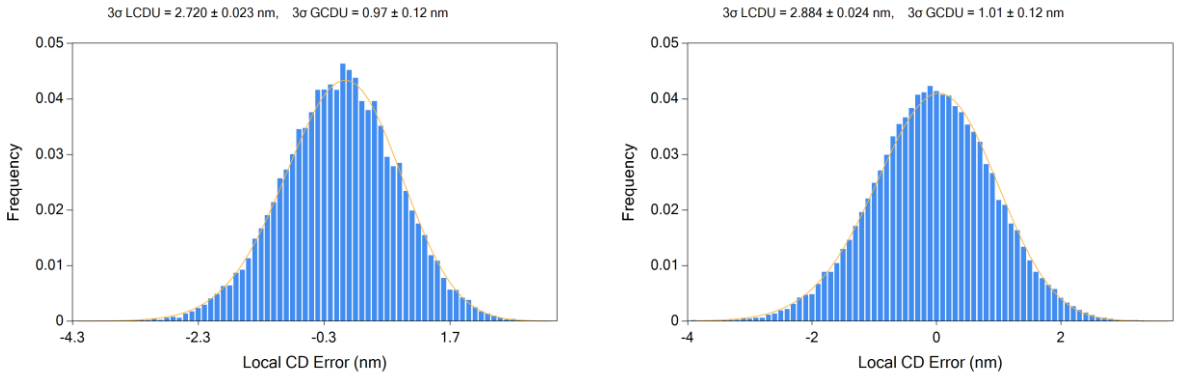

(a) (b)

Figure 5. Histograms of local CD error after removal of the systematic across-SEM-field variations from Figure 4 for (a) Run 1, and (b) Run 2 using the first sampling plan (aligned to the array corner) and horizontal pitch = 80 nm, vertical pitch = 46 nm. The local CD error comes from 202 holes measured in one image relative to the mean of that image (after removal of the systematic across-SEM-field sigmature), then combined with the results from all 144 images.

Finally, Runs 1 and 2 were compared by subtracting the CDs from the two runs on a matched hole-by-hole basis. Because each image was aligned using the corner of the hole array, the exact same holes were measured in each image. Thus, it was possible to automatically subtract each pair of CD values and look at the distribution of resulting differences. Figure 6 is a plot of the result and an indication of the random metrology error when measuring a single contact hole. The mean CD difference between the two runs was 0.215 nm, reflecting the impact of the CD-SEM electron dose on the photoresist. The standard deviation of the difference was 0.315 nm, with a maximum difference of 1.7 nm and a minimum difference of -1.2 nm. The uncertainty in the measurement of one hole CD due to metrology is estimated using the standard deviation of this distribution divided by $\sqrt{2}$.

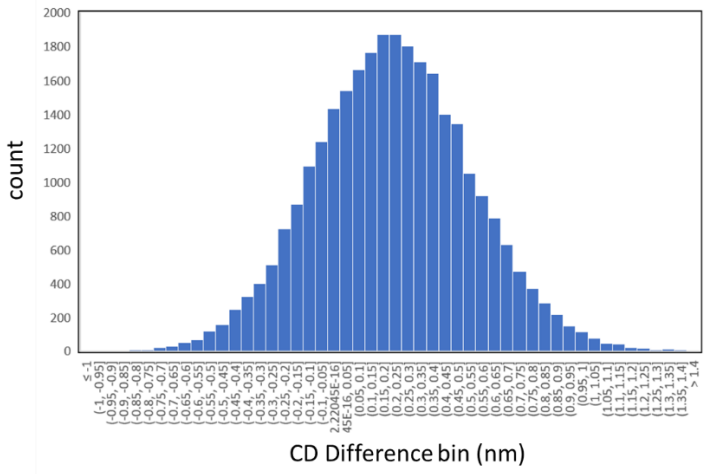

Figure 6. Histogram of the results of matched hole-by-hole differencing of the CD values obtained from Runs 1 and 2. The mean CD difference between the two runs was 0.215 nm and standard deviation of the difference was 0.315 nm.

Table I provides a summary of the results so far. The total CDU is the sum (in quadrature) of the original local and global CDU (systematic errors included). The final local CDU, showing the imaging and resist contribution to the stochastics, subtracts (in quadrature) the measured random metrology uncertainty from the local CDU that was obtained after the removal of the systematic across-SEM-field signature.

The second sampling plan looked at 50 different points in a single scanner field, each measurement far away from the edge of the array of holes (thus reducing the possibility of optical proximity effects). These 50 points in the field came from 50 different points on the mask, so stochastic mask-making variations would be approximately averaged away. The resulting systematic across-SEM-field signature would thus be the contribution of the CD-SEM only. This result is found in the middle plot of Figure 7. Subtracting the SEM only across-SEM-field signature obtained from sampling plan 2 from the SEM + Mask signature of sampling plan 1 produces a signature of the systematic mask contribution to sampling plan 1. Notice that the SEM-only signature shows a slowly varying signature as expected for systematic CD-SEM variation across the field. The mask-only result, on the other hand, shows very little discernable pattern, indicating that the stochastic errors in the mask-making process likely produced this signature. It is also interesting to note that the mask-only systematic variation is larger than the SEM+mask combined, indicating that for this specific case the CD-SEM systematic errors are canceling out some of the mask systematic errors. Table II provides a summary of these results.

Table I. Summary of sources of variation decomposition for sampling plan 1, with images aligned to the corner of the array, for H80V46. Uncertainty estimates provided here are ± two standard errors.

	Run 1 (3σ, nm)	**Run 2 (3σ, nm)**
Total CDU	3.27 ± 0.03	3.45 ± 0.03
Local CDU (systematics included)	3.12 ± 0.03	3.30 ± 0.03
Global CDU	0.97 ± 0.11	1.01 ± 0.12
Across-SEM-Field (SEM + mask)	1.53	1.61
Local CDU (systematics removed)	2.72 ± 0.02	2.88 ± 0.02
Repeat Metrology Variation/$\sqrt{2}$	0.668 ± 0.006	0.668 ± 0.006
Stochastics Only LCDU	2.64 ± 0.02	2.80 ± 0.02

Table II. Comparing the two sampling plans produces further analysis of the contributors to across-SEM-field errors.

	3σ (nm)
Across-SEM-Field (SEM + mask)	1.61
Across-SEM-Field (SEM only)	1.09
Across-SEM-Field (mask only)	1.73

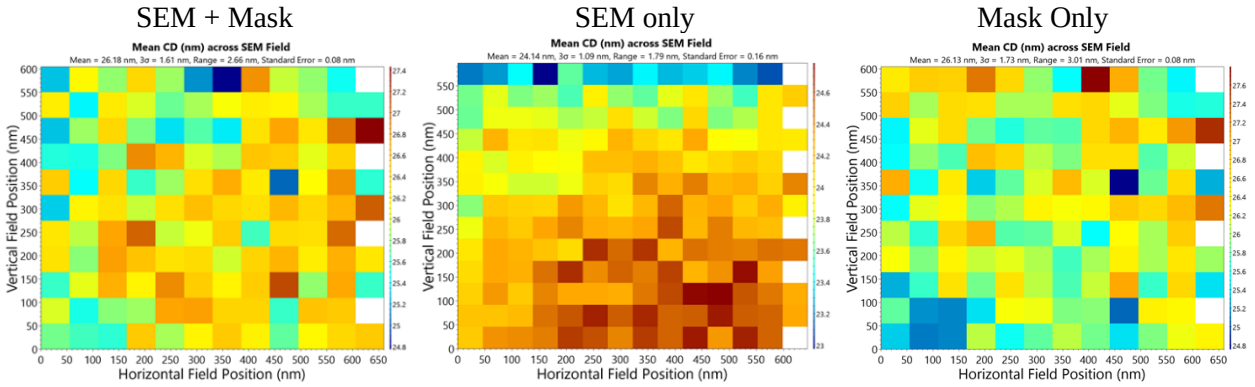

Figure 7. Subtracting the SEM only across-SEM-field signature obtained from sampling plan 2 from the SEM + Mask signature of sampling plan 1 produces a signature of the systematic mask contribution to sampling plane 1.

The results above are for the H80V46 pitch case. Similar results can be obtained for the two other pitches (H70V40 and H66V38). Those results are provided in Tables III and IV. It is interesting to observe that in all cases Run 2 exhibits about 8% greater variability than Run 1. It seems likely that the effect of the electron dose during the first SEM measurement (Run 1) is to add variability to the CD as measured in the second run.

IV. CONCLUSIONS

For EUV contact hole printing near the limits of resolution, stochastics is generally the dominant source of critical dimension variability. In this study, staggered arrays of holes with diagonal pitches ranging from 46 – 56 nm were analyzed with a bottoms-up sources of variation approach. An original 3.3 nm of total 3σ CDU (for the H80V46 pitch case using the corner-aligned sampling plan) was decomposed into 2.6 nm of pure stochastic variation, 1.7 nm of systematic mask variation, 1.0 nm of systematic across-SEM-field metrology error, 1.0 nm of global CDU (only across-wafer; across-scanner field was not measured), and 0.7 nm of random metrology error. The combined systematic mask + metrology error was 1.6 nm, which can be subtracted directly from the measurements of every image.

It is common to observe that repeat metrology error is relatively small. In this case the local CDU is reduced from 2.7 nm to 2.6 nm when the random metrology error is removed. Often, this amount of correction is small enough to be ignored (or possibly approximated using typical values rather than measured values). The systematic metrology error (that is, the systematic across-SEM-field variation) is larger, with a larger impact on the results. Additionally, the systematic across-SEM-field variation is easier to measure and subtract off (especially if this step is automated), regardless of whether a mask-aligned or random mask position sampling plan is used.

Finally, the goal of automating the decomposition steps has been realized using MetroLER, with consequent reduction in time spent and the possibility of mistakes.

Table III. Summary of sources of variation decomposition for sampling plan 1, with images aligned to the corner of the array, for H70V40. Uncertainty estimates provided here are ± two standard errors.

	Run 1 (3σ, nm)	**Run 2 (3σ, nm)**
Total CDU	3.00 ± 0.02	3.20 ± 0.02
Local CDU (systematics included)	2.88 ± 0.02	3.07 ± 0.02
Global CDU	0.86 ± 0.10	0.90 ± 0.12
Across-SEM-Field (SEM + mask)	1.58	1.67
Local CDU (systematics removed)	2.40 ± 0.02	2.58 ± 0.02
Repeat Metrology Variation/$\sqrt{2}$	0.71 ± 0.01	0.71 ± 0.01
Stochastics Only LCDU	2.29 ± 0.02	2.48 ± 0.02

Table IV. Summary of sources of variation decomposition for sampling plan 1, with images aligned to the corner of the array, for H66V38. Uncertainty estimates provided here are ± two standard errors.

	Run 1 (3σ, nm)	**Run 2 (3σ, nm)**
Total CDU	3.12 ± 0.02	3.35 ± 0.02
Local CDU (systematics included)	2.98 ± 0.03	3.21 ± 0.02
Global CDU	0.92 ± 0.11	0.97 ± 0.11
Across-SEM-Field (SEM + mask)	1.70	1.82
Local CDU (systematics removed)	2.45 ± 0.02	2.65 ± 0.02
Repeat Metrology Variation/$\sqrt{2}$	0.71 ± 0.01	0.71 ± 0.01
Stochastics Only LCDU	2.35 ± 0.02	2.55 ± 0.02

References

[1] Chris A. Mack, Fundamental Principles of Optical Lithography: The Science of Microfabrication, p. 312, John Wiley & Sons, London (2007).

[2] Gian F. Lorusso, Ming Mao, Liesbeth Reijnen, Katja Viatkina, Roel Knops, Gijsbert Rispens, Timon Fliervoet, "Influence of etch process on contact hole local critical dimension uniformity in extreme-ultraviolet lithography", Proc. SPIE 9425, Advances in Patterning Materials and Processes XXXII, 94250K (2015).

[3] Lieve Van Look, Joost Bekaert, Andreas Frommhold, Eric Hendrickx, Gijsbert Rispens, and Guido Schiffelers "Optimization and stability of CD variability in pitch 40 nm contact holes on NXE:3300", Proc. SPIE 10809, International Conference on Extreme Ultraviolet Lithography 2018, 108090M (2018).

[4] Gian F. Lorusso, Gijsbert Rispens, Vito Rutigliani, Frieda Van Roey, Andreas Frommhold, Guido Schiffelers, "Roughness decomposition: an on-wafer methodology to discriminate mask, metrology, and shot noise contributions", Proc. SPIE 10959, Metrology, Inspection, and Process Control for Microlithography XXXIII, 109590T (2019).

[5] Douglas C. Montgomery, Design and Analysis of Experiments, 4th edition, Chapter 12, John Wiley & Sons, New York (2009).